IET Science, Measurement & Technology

Research Article

IET Journals
The Institution of Engineering and Technology

Prediction of radiated emissions from high-speed printed circuit board traces using dipole antenna and imbalance difference model

ISSN 1751-8822
Received on 25th January 2015
Revised on 16th July 2015
Accepted on 14th August 2015
doi: 10.1049/iet-smt.2015.0019
www.ietdl.org

Mohamad Zarar Mohd Jenu, Ahmed Mohammed Sayegh ✉

Research Center for Applied Electromagnetics, Universiti Tun Hussein Onn Malaysia, Batu Pahat, Johor, Malaysia
✉ *E-mail: ahmed_su2008@yahoo.com*

Abstract: The ever-increasing clock speeds on printed circuit board (PCB) have enhanced PCB traces to become efficient radiators of electromagnetic energy. Conventionally, the radiated emissions (REs) of electrically short PCB traces are estimated using expressions developed based on electric/magnetic dipole antenna. In this study, a novel method was proposed to estimate RE from electrically long PCB traces. In this method, the differential-mode (DM) RE was estimated using the transmission-line theory and dipole antenna model, whereas the common-mode (CM) RE was computed by a combination of imbalance difference model and a dipole antenna. Conceptually, the electrically long trace was chunked into multiple electrically short segments and the fields of each segment were superimposed to obtain the net radiated fields. Additionally, closed-form expressions were derived to estimate the DM REs from electrically long PCB traces based on dipole antenna model. On the other hand, CM RE was predicted by line integration of CM current distribution which was approximated using imbalance difference model and asymmetrical dipole antenna model. The effectiveness of the proposed method was verified using compact single-sided PCB by comparing the computed results with the measured results taken in a semi-anechoic chamber, and a good agreement with accuracy more than 90% was observed for upper bounds of the REs.

1 Introduction

The ever-increasing clock speed on printed circuit board (PCB) to several gigahertz has enhanced PCB traces to become efficient radiators of electromagnetic energy. Naturally, PCB traces can generate both differential-mode (DM) and common-mode (CM) radiated emissions (REs) which are produced due to DM and CM currents, respectively. Although CM current is typically much less than DM current, the CM RE value is much greater than that of DM current [1–3]. Hence, properly designed PCBs can offer a cost-effective approach to achieve electromagnetic compatibility (EMC) compliance. Hence, the consideration of EMC during the design phase is becoming critically important.

Although DM/CM RE have been estimated successfully using expressions in [2], those expressions are not applicable for electrically long traces where the trace length becomes comparable with the wavelength since they are derived based on Hertzian dipole antenna where the current is assumed to be uniform along the trace. Additionally, the estimation of CM RE using that expression involves the measurement of CM current using current probe which is a tedious task due to the dependency of CM current on position and frequency. Later, in other studies, the DM RE is estimated using closed-form expression that is elaborated based on a transmission-line model and modified Green's function [4, 5]. However, it requires intensive computation to compute all radiated fields in the entire sphere.

In this paper, an alternative approach is proposed for estimating both DM and CM RE from PCB traces. First, DM RE is predicted by dividing the electrically long trace into many electrically short segments. Then, the RE from each short segment is computed using the formulation described in [2] for DM RE. Although this method provides accurate results, it is a time-consuming method due to the massive calculation of RE for all segments. Therefore, a closed-form expression is derived based on dipole antenna and transmission-line theory for predicting the maximum DM RE from PCB traces as shown in Section 2.

Secondly, a novel approach is presented for estimating CM RE from PCB traces by a combination of imbalance difference model and asymmetrical dipole antenna in Section 3. The imbalance difference model explains how the DM signals can induce CM signals on the nearby metallic structures [6]. Although imbalance difference model has been demonstrated successfully in identifying and quantifying CM voltage sources at the junctions where the imbalance change occurs [7], it is never adopted before for estimating CM RE from PCB traces but asymmetrical dipole model has been adopted for estimating CM RE in several studies before [8–11]. Such studies have investigated the CM RE not from PCB traces but from the cables attached to a conductive enclosure. In this paper, the imbalance difference model is used to locate and quantify the CM voltage source on the PCB while the signal trace and the ground plane in microstrip PCB are modelled as asymmetrical dipole antenna. The CM current is approximated using the identified CM voltage and the input impedance of the asymmetric dipole. Then, the maximum CM RE can be predicted once the CM current distribution on the dipole arms is known.

Quantitatively, this method would be acceptable from the design point of view if the error between analytical modelling and the measurement do not exceed 10% in the worst case. However, in this paper, this method has provided results with accuracy about 90.07% in loaded circuit configuration as a practical case. For an actual complex PCB that are populated with several traces, this method can be used to estimate the total RE by computing the RE for each trace, and then the net RE can be computed as the superposition of all radiated fields from all traces. However, in this research work, a single-sided PCB is employed to verify the proposed method. The overall RE is calculated as the total sum of DM and CM RE. The computed results of total REs are then validated and compared with the total results of PCB RE which is taken from the semi-anechoic chamber (SAC) and good agreements are obtained between the two results. This paper is structured as follows: Section 2 shows the estimation of DM RE dipole antenna and the transmission-line theory. In Section 3, the CM RE is estimated based on imbalance difference theory and asymmetrical dipole antenna. Section 4 describes the PCB under test for measurement of SAC. In Section 5, the obtained predicted

results are presented, discussed, analysed, and verified by comparing it with the results measured in SAC.

2 Prediction of DM REs from high-speed PCB traces

The maximum DM electric field, $|\hat{E}_D|_{max}$ from two parallel signal and the return traces on PCB is given as in [2]

$$|\hat{E}_D|_{max} = \frac{1.316 \times 10^{-14} \, |\hat{I}_D| \, f^2 \, l \, s}{r} \tag{1}$$

where $|\hat{I}_D|$ denotes the DM current magnitude, f is the frequency, l is the length of signal trace, s is the distance between signal trace and return trace, and r is the distance to the observation point.

Although (1) provides good estimation for DM RE, it is not applicable for electrically long traces since it is derived based on Hertzian dipole antenna. As a solution, the long trace can be divided into electrically short segments as shown in Section 2.1.

2.1 Prediction of DM-RE from PCB traces using trace segmentation method

The computation of total DM RE of electrically long trace requires dividing the trace into multiple electrically short segments, each with a length of Δx according to the wavelength of the maximum frequency of interest as shown in Fig. 1. Then, the DM RE from each segment will be estimated using (1). Once the DM current is known for each trace, the total radiated field can easily be computed by superimposing the fields generated by both traces. Therefore, it is necessary to compute the DM current for the estimation of DM RE.

One method to calculate the DM current for electrically long traces is by applying the transmission-line theory as in [12]

$$\hat{I}(f, x) = V_s(f)(A + B)/(C + D) \tag{2}$$

where

$$A = Z_0 \cos[\beta(l - x)] \tag{3}$$

$$B = jZ_L(f) \sin[\beta(l - x)] \tag{4}$$

$$C = Z_0[Z_s(f) + Z_L(f)] \cos(\beta l) \tag{5}$$

$$D = j[Z_0^2 + Z_s(f) \, Z_L(f)] \sin(\beta l) \tag{6}$$

$V_s(f)$ is the source of voltage exciting the line, Z_0 is the characteristic impedance of the line, β is the phase constant, λ is the wavelength at frequency f, v is the propagation velocity in the line, and ε_e is the equivalent relative dielectric constant of the line. The line input impedance, $Z_{in}(f)$ can be written as in [13]

$$Z_{in}(f) = Z_0(E + F)/(G + H) \tag{7}$$

where

$$E = Z_L(f) \cos(\beta l) \tag{8}$$

$$F = jZ_0(f) \sin(\beta l) \tag{9}$$

$$G = Z_0(f) \cos(\beta l) \tag{10}$$

$$H = jZ_L(f) \sin(\beta l) \tag{11}$$

2.2 Prediction of DM RE from PCB traces using long dipole antenna

The basic technique of estimating the radiated fields of two parallel traces is by summing up the radiated fields of each trace. This method considers each trace as a dipole antenna and superimposes the fields of each trace to compute the net radiated field which is virtually identical to the calculation of the radiated fields of an array of Hertzian dipole antennas [13].

The total radiated electric field is the sum of each radiated electric field as shown in Fig. 2, and is given by [2]

$$|\hat{E}_\theta| = \hat{M}\left[\frac{\hat{I}_1}{r_1} e^{-j\beta_0 r_1} + \frac{\hat{I}_2}{r_2} e^{-j\beta_0 r_2}\right] \tag{12}$$

where $\hat{I}_1$, $\hat{I}_2$ are the DM currents of antenna, $\hat{M}$ is a function which depends on the antenna type.

The function $\hat{M}$ [2] for long dipole antenna is given as

$$\hat{M} = j60 \, F(\theta) \tag{13}$$

where

$$F(\theta) = \frac{[\cos(\pi l/\lambda_0) \cos(\theta)] - \cos(\pi l/\lambda_0)}{\sin(\theta)} \tag{14}$$

From Fig. 2

$$r_1 = r - s \cos(\phi) \tag{15}$$

$$r_2 = r + s \cos(\phi) \tag{16}$$

In this method, the distance between the device under test (DUT) and the receiving antenna is about ten wavelengths at the maximum frequency of interest (1 GHz) which is reasonably acceptable to assume the radial distances r_1 and r_2 are parallel to each other based on far-field, parallel-ray approximation. This assumption is a

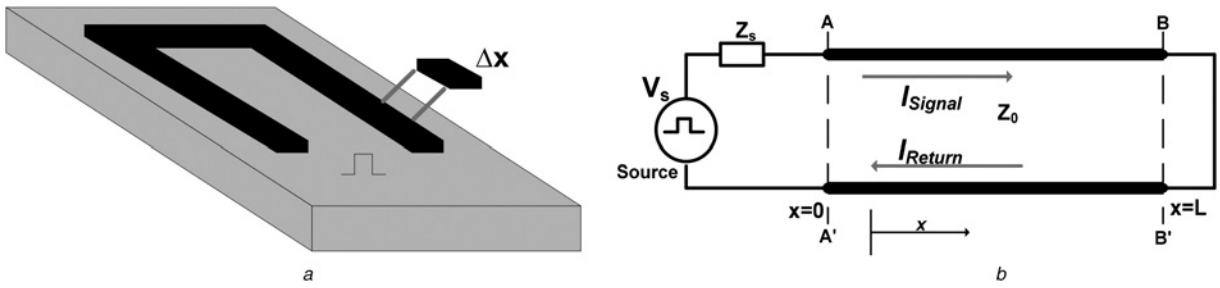

Fig. 1 *Prediction of DM-RE from PCB traces using trace segmentation method*

a Single-sided PCB with two parallel traces in short-circuit mode
b Equivalent circuit for two parallel traces

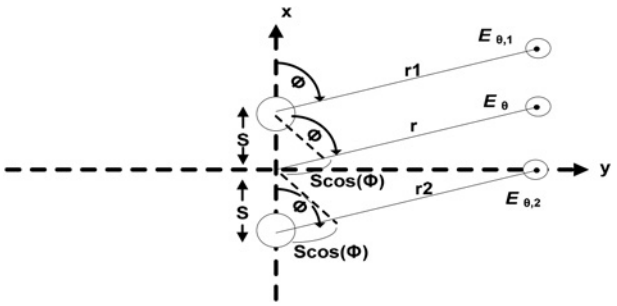

Fig. 2 *Calculation of the far-fields of two parallel long wire currents*

reasonable approximation to avoid the complexity of computational process where the denominators can be assumed as the same variable $r = r_1 = r_2$. This assumption is avoided when the signal phase changes as the distance changes. Therefore, the terms $e^{-j\beta_0 r_1}$, $e^{-j\beta_0 r_2}$ are substituted differently. In other words, this assumption can be applied only on the terms related to physical distance and must be avoided in electrical distance dependent calculations. Substituting (15) and (16) into (12) then inserting $r_1 = r$ and $r_2 = r$ in the denominators gives

$$|\hat{E}_\theta| = A\left[\hat{I}_1 e^{j\beta_0 S\cos(\phi)} + \hat{I}_2 e^{-j\beta_0 S\cos(\phi)}\right] \tag{17}$$

where $A = (\hat{M}/r)\, e^{-j\beta_0 r}$.

The result in (17) can be presented in a special form for the case of DM currents $\hat{I}_1 = I_D$ $I_1 = I_D$, and $I_2 = -I_D$. The radiated fields can be determined, under the assumption of sinusoidal current distributions since the digital signal can be decomposed into a series of sinusoidal signals (harmonics) by treating each trace as a long dipole and substitute (12) into (17). Moreover, we substitute $\emptyset = 0$ (so that the fields are in the same plane as the wires). Consequently, the maximum RE expression can be derived as follows:

$$|\hat{E}_D|_{max} = A\left[\hat{I}_1\, e^{j\beta_0 S\cos(\phi)} - \hat{I}_2\, e^{-j\beta_0 S\cos(\phi)}\right] \tag{18}$$

$$= \frac{120}{r}|\hat{I}_D|\ \sin(\beta_0 S)\, e^{-j\beta_0 r}\, F(\theta) \tag{19}$$

$$= \frac{-120}{r}\ |\hat{I}_D|\ \beta_0 S\, e^{-j\beta_0 r}\, F(\theta) \tag{20}$$

$$\text{for } \beta_0 S \ll 1$$

By substituting, $\beta_0 = 2\pi f/v_0 = 2.1 \times 10^{-8} f$, the magnitude of (20) can be given as

$$|\hat{E}_D|_{max} = 2.52 \times 10^{-6}\frac{|\hat{I}_D|\, f\, S}{r} F(\theta) \tag{21}$$

For measurement in 3 m SAC ($r = 3$), (21) becomes

$$|\hat{E}_D|_{max} = 8.4 \times 10^{-7}|\hat{I}_D|\, f\, S\, F(\theta) \tag{22}$$

where

$$F(\theta) = \frac{\cos[\cos\ \theta(\pi\, l/\lambda_0)] - \cos\ (\ \pi\, l/\lambda_0)}{\sin\ \theta} \tag{23}$$

As a special case, the maximum DM RE from trace with maximum length of one wavelength is obtained at $\theta = 90^\circ$, thus

$$|\hat{E}_D|_{max} = 2.52 \times 10^{-6}\frac{|\hat{I}_D|\, f\, S}{r}[1 - \cos\ (\ \pi\, l/\lambda_0)] \tag{24}$$

Equation (24) was employed to estimate the possible maximum DM RE of electrically long PCB traces. It is observed that (22) is similar to (1), which is used for electrically short segments. However, this approach is valid as the operating frequency does not exceed the maximum frequency within the quasi-transverse electromagnetic (TEM) frequency range which is given as in [12]

$$f[\text{GHz}] \simeq \frac{21.3}{(w[\text{mm}] + 2t[\text{mm}])\sqrt{\varepsilon_r} + 1} \tag{25}$$

where t is the dielectric thickness, ε_r is the relative dielectric permittivity, and w is the trace width.

3 Prediction of CM REs from high-speed PCB traces

The maximum CM RE from PCB traces can be estimated using a simple expression which has been derived in [2] based on the electric dipole as

$$|\hat{E}_D|_{max} = \frac{1.257 \times 10^{-6}\ |\hat{I}_C|\, f\, l}{r} \tag{26}$$

where $|\hat{I}_C|$ denotes the CM current. Even though (26) estimates the CM REs reasonably, it is only applicable to electrically short traces in which the currents are assumed constant. Therefore, the maximum CM RE for electrically long traces can be estimated using a dipole model. The same steps from (12) to (17) can be applied with replacing $\hat{I}_1 = \hat{I}_C$ and $\hat{I}_2 = \hat{I}_C$, then the maximum CM RE is written as

$$|\hat{E}_C|_{max} = \frac{120|\hat{I}_C|}{r}\ \left[1 - \cos\left(\frac{\pi l}{\lambda_0}\right)\right] \tag{27}$$

For $r = 3$ m, (27) becomes

$$|\hat{E}_C|_{max} = 40|\hat{I}_C|\left[1 - \cos\left(\frac{\pi l}{\lambda_0}\right)\right] \tag{28}$$

Although these closed-form expressions estimate the CM RE accurately, it provides inaccurate results for traces which are longer than one wavelength. Thus, a novel method is proposed based on the imbalance difference theory and asymmetrical dipole antenna as in Section 3.1.

3.1 Imbalance difference model for estimating CM RE

Watanabe *et al.* [6] have proven that an electrical imbalance of a PCB circuit does not necessarily result in CM RE. Instead, CM voltage source can be identified at the point where the changes of imbalance occur. Briefly, the computational process involves replacing DM sources with corresponding CM sources at the junctions where imbalance changes. The imbalance difference factor, h can be defined as the ration between the CM current on the signal trace and the total CM current. For microstrip PCB structure, it can be given in a form of stray capacitance for the trace (C_{trace}) and ground plane C_{board} as in [6]

$$h = \frac{I_{CM\text{-}signal}}{I_{CM\text{-}total}} = \frac{C_{trace}}{C_{trace} + C_{board}} \tag{29}$$

The stray capacitance of the trace and ground plane can be computed either using closed-form expressions [14] or by using an electromagnetic simulation such as quasi-three-dimensional extractor. Once the stray capacitances are known, the CM voltage at the point where the imbalance changes can be expressed as in [6]

$$V_{CM}(x) = \Delta h\ V_{DM}(x) = (h_2 - h_1)\ V_{DM}(x) \tag{30}$$

IET Sci. Meas. Technol., 2016, Vol. 10, Iss. 1, pp. 28–37

where h_2 is the imbalance factor for PCB trace, $h_1 = 0$ because there is no trace after the junction between the DM source and the signal trace. Therefore, (30) can be re-written as

$$V_{\mathrm{CM}}(0) = h_2 V_{\mathrm{DM}}(0) = \frac{C_{\mathrm{trace}}}{C_{\mathrm{trace}} + C_{\mathrm{board}}} V_{\mathrm{DM}}(0) \tag{31}$$

3.2 Estimation of CM current distribution using asymmetrical dipole antenna

The properties of asymmetrical dipole antenna have been widely described in many published works. The current distribution of the asymmetrical long dipole antenna is not constant but changes with positions. However, the CM current distribution on the asymmetrical dipole has been estimated in many works as in [15, 16]. In this paper, the CM current distribution is estimated according to Schelkunoff and Friis approach as in [17].

Referring to Fig. 3, the asymmetrical antenna can be virtually decomposed into two symmetrical dipole antennas. Therefore, each branch can be analysed independently since the geometrical dimensions and CM voltage/current are different. According to [8, 17], the CM current distribution on the two arms of the dipole antenna can be computed as

$$I_1(x) = \frac{4\pi V_1}{\psi_1 \eta} \times \frac{\sin\beta(l_1 - |x|) + M_1(l_1, x)/\psi_1}{\cos\beta l_1 + A_1(l_1)/\psi_1}, \quad 0 < x < l_1 \tag{32}$$

$$I_2(x) = \frac{4\pi V_2}{\psi_2 \eta} \times \frac{\sin\beta(l_2 - |x|) + M_2(l_2, x)/\psi_2}{\cos\beta l_2 + A_2(l_2)/\psi_2}, \quad -l_2 < x < 0 \tag{33}$$

where $\psi_1 = 2\ln(2l_1/a)$, $\psi_2 = 2\ln(2l_2/b)$, η is the impedance of the free space which is equal to 377 Ω, l_1 and l_2 are the half-lengths of the asymmetrical antenna which are equivalent to the trace length and the board length, respectively, and the functions of $M(l, x)$ and $A(l)$ are given in [15]. The cylindrical arms of asymmetrical dipole have radii of a and b which are equal to one quarter of the signal trace width ($w1$) and the board width ($w2$), respectively. The CM voltage can be estimated by applying the voltage divider rule for the input impedance of each part as

$$V_1 = V\frac{Z_1}{Z_1 + Z_2}, \quad V_2 = V\frac{Z_2}{Z_1 + Z_2} \tag{34}$$

where the input impedances Z_1 and Z_2 are computed as

$$Z_1 = \frac{V_1}{I_1(x=0)}, \quad Z_2 = \frac{V_2}{I_2(x=0)} \tag{35}$$

3.3 Estimation of maximum CM RE using dipole antenna model

Since the CM current is computed using (32) and (33), the CM RE can be estimated using the equivalent asymmetrical dipole antenna. As mentioned before, the long dipole is divided into many short segments. The CM RE from this segment is given as in [13]

$$\mathrm{d}E_\theta = \frac{\eta\beta I(x)\mathrm{e}^{-\mathrm{j}\beta r_1}}{4\pi r_1} \sin\theta_1 \,\mathrm{d}x \tag{36}$$

where r_1, θ_1 are the radial distance and angle at position x. As shown in Fig. 4a, they can be given as

$$r_1 = \sqrt{(r^2 + x^2 - 2rx\cos\theta)}, \quad \sin\theta_1 = \frac{r\sin\theta}{r_1} \tag{37}$$

The CM RE from the dipole antenna is then estimated using line integration of the CM current along the dipole arms as in [13]

$$E_\theta = \frac{\eta\beta}{4\pi}\sin\theta \times \left\{\int_0^{l_1} \frac{I_1(x)\,\mathrm{e}^{-\mathrm{j}\beta r_1}}{{r_1}^2}\mathrm{d}x + \int_{-l_2}^{0} \frac{I_2(x)\,\mathrm{e}^{-\mathrm{j}\beta r_1}}{{r_1}^2}\,\mathrm{d}x\right\} \tag{38}$$

In fact, the maximum CM RE corresponding to each frequency is obtained at certain angle, $\theta_{\max}$ which can be computed using iterative calculation for all the values of θ at the range from 0° to 180°. However, a special case can be obtained when the trace and its return paths are identical. If the signal trace and the return trace are identical and electrically balanced (stray capacitances are equal, $C_{\mathrm{trace}} = C_{\mathrm{board}}$), the value of imbalance difference factor h_2 is 0.5. This means the CM current is equally distributed between the signal trace and return trace as shown in Fig. 4b. It can be modelled clearly as a symmetrical dipole. Therefore, a single-sided PCB with two identical signals and return traces has been used as a compact DUT to avoid the complexity of PCB structure as illustrated in Section 4. Such dipole as illustrated in Fig. 4b is represented by inductance, L_t which is equally distributed on the two arms. In addition, a parasitic capacitance C_t is created between

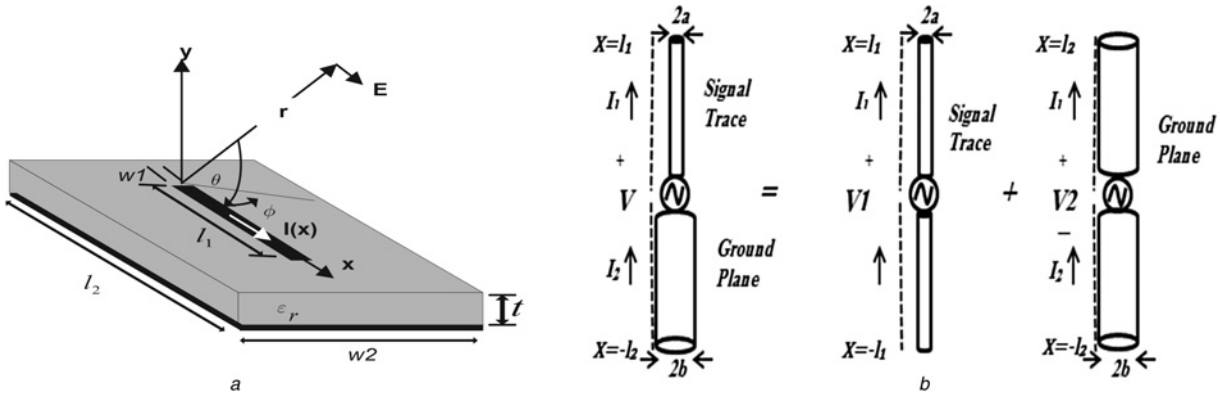

Fig. 3 *Estimation of CM current distribution using asymmetrical dipole antenna*

a Simple microstrip PCB structure

b Equivalent CM model based on asymmetrical dipole antenna

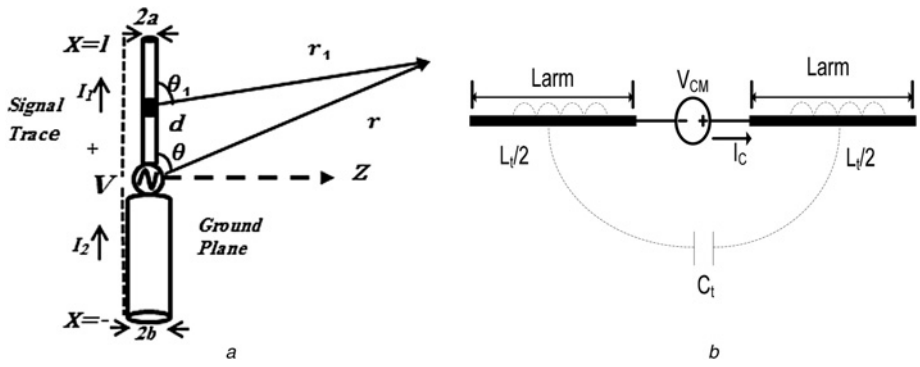

Fig. 4 *Estimation of maximum CM RE using dipole antenna model*

a Equivalent asymmetrical dipole model for CM RE
b Equivalent symmetrical dipole of CM circuit

the two arms. In reality, these arms are the two parallel traces on the PCB under test

$$L_{\mathrm{t}} = \frac{\mu_0 l_{\mathrm{d}}}{3\pi}\left[\ln\left(\frac{2l_{\mathrm{d}}}{a}\right) - \frac{11}{6}\right] \tag{39}$$

$$C_{\mathrm{t}} = \frac{\varepsilon_{\mathrm{e}}\varepsilon_0 l_{\mathrm{d}}\ \pi}{D} \tag{40}$$

where total dipole length $l_{\mathrm{d}} = 2L_{\mathrm{arm}}$, a is the radius of trace, μ_0 and ε_0 are free space permeability and permittivity, respectively, and finally

$$D = \ln\left(\frac{2l_{\mathrm{d}}}{a}\right) \tag{41}$$

The radiation resistance $R_{\mathrm{rd}}(f)$ is frequency-dependent [11] and demarcated as

$$R_{\mathrm{rd}}(f) = \begin{cases} 80\pi^2\left(\dfrac{l_{\mathrm{d}}}{\lambda}\right), & L_{\mathrm{arm}} \le \lambda/4 \\ 73\ \Omega, & L_{\mathrm{arm}} > \lambda/4 \end{cases} \tag{42}$$

The phasor CM current, $\hat{I}_{\mathrm{c}}(f)$ can be subsequently expressed as in [12]

$$\hat{I}_{\mathrm{C}}(f) = \frac{\hat{V}_{\mathrm{CM}}}{R_{\mathrm{rd}}(f) + \mathrm{j}\left(\omega L_{\mathrm{t}} - (1/\omega C_{\mathrm{t}})\right)} \tag{43}$$

The calculation of CM current depends primarily on the CM voltage which can be identified and quantified based on the imbalance difference concept. With known CM current, the CM radiation can be computed. Ultimately, DM and CM radiated fields are superimposed to give the total PCB REs.

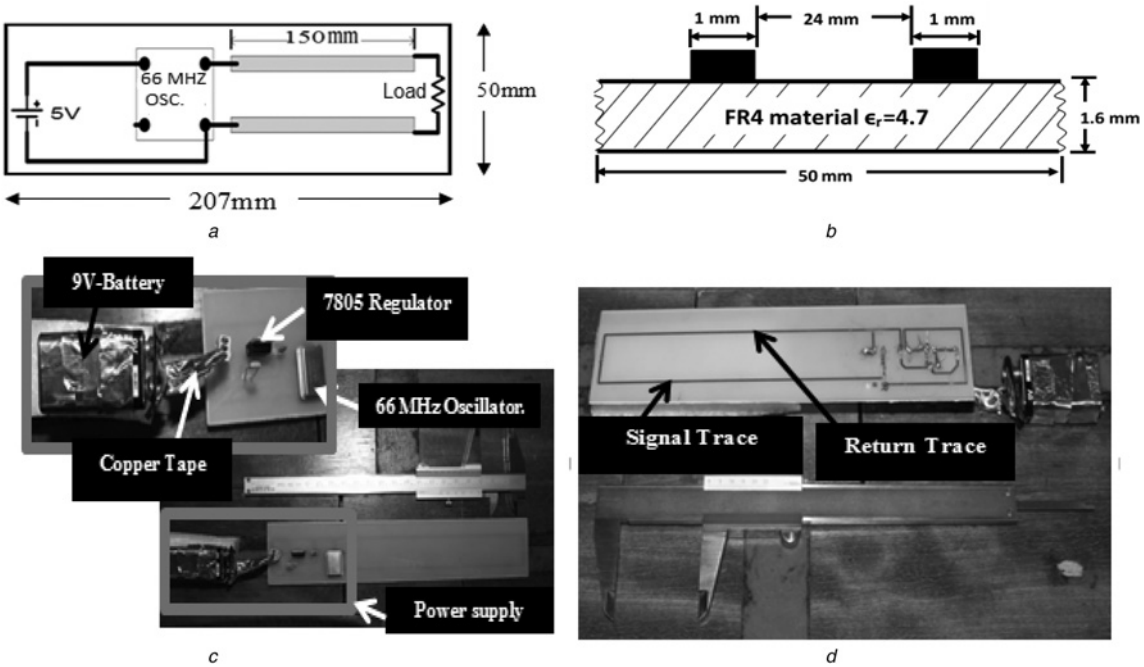

Fig. 5 *Description of PCB under test in SAC for measurement set-up*

a Schematic layout
b Cross-sectional dimensions of PCB under test
c Top view
d Bottom view of DUT

IET Sci. Meas. Technol., 2016, Vol. 10, Iss. 1, pp. 28–37

4 Description of PCB under test in SAC for measurement set-up

Names in order to verify the proposed method for estimating the RE from PCB traces, a simple single-sided PCB was constructed as shown schematically in Fig. 5a. This 5 cm × 20.7 cm PCB was fabricated such that the signal trace of 1 mm wide and 15 cm long was positioned at an offset of 12 mm from the centre of the board. The return trace was on the same side, as the signal trace, as shown in Fig. 5*b*. Both traces were etched on a 1.6 mm thick FR4 dielectric material. The signal trace was driven by a 66 MHz trapezoidal signal which has an amplitude of 5 V, 50% duty ratio, and 6 ns rise/fall time. A battery power supply consists of 9 V battery and 7805 regulator provides 5 V dc to the 66 MHz oscillator. The output pin of the oscillator was connected to the near-end of the signal trace as shown in Figs. 5*c* and *d*. The load was configured into three distinct conditions: short, open, and 100 Ω resistance. It is important to note that the PCB under test was designed to be as compact as possible to avoid the extra RE that may be emitted from the oscillator or any other related dc connections. To ensure that the RE is produced only from the signal traces, a metallic box with 30 cm × 30 cm × 12 cm was used to shield the power supply part including the regulator, oscillator, and their related connection traces as shown in Figs. 6*a* and *b*.

The PCB REs were measured in SAC facility at Universiti Tun Hussein Onn Malaysia (UTHM) that is regularly used for EMC qualification testing. The DUT was placed on a 0.8 m tall wooden table above the ground plane in SAC and rotated 360° to detect the maximum RE. A log-periodic antenna was employed to measure the RE in the frequency range from 30 MHz to 1 GHz as shown in Fig. 6*c*. The distance between the PCB under test and the receiving antenna was about 3 m while the electromagnetic interference receiver was located outside the chamber to record the maximum RE as the table rotates 360°.

Although in this paper a single-sided PCB was employed as DUT, this method still can be used to estimate RE from the multilayer used but with more complexity of modelling and calculation using the general proposed model in Sections 2 and 3. For actual PCB, this method can also be used for all the traces and then compute the total RE due to all traces.

5 Results and discussion

5.1 Prediction of PCB DM and CM currents

In this paper, a MATLAB R2010a software was employed to perform all calculations of DM and CM RE. The DM and CM currents were estimated according to the foregoing techniques. Three operating modes (short circuit, open circuit, and 100 Ω load) were examined, analysed, and compared. The corresponding results are presented in Fig. 7. For all the operating modes, DM current was found to be much greater than CM current. Such observation is unsurprising as we know that DM current is a functional current in the circuit, whereas CM current exists due to the imbalance of PCB structure.

For short-circuit configuration (Fig. 7*a*), the DM current declined abruptly but the CM current decreased gradually with frequency. In case of open-circuit configuration (Fig. 7*b*), the DM current was still higher than the CM current as a result of the capacitance between two parallel traces. This open-circuit DM current was, nonetheless, lower than short-circuit DM current. As for 100 Ω load configuration (Fig. 7*c*), the DM current dropped rapidly, whereas the CM current diminished slowly as the frequency increased. The DM current for this configuration was comparable with that of a short circuit but was higher than the open-circuit DM current. Notably, DM current was reduced to 0 dB in short-circuit configuration but not for the other two.

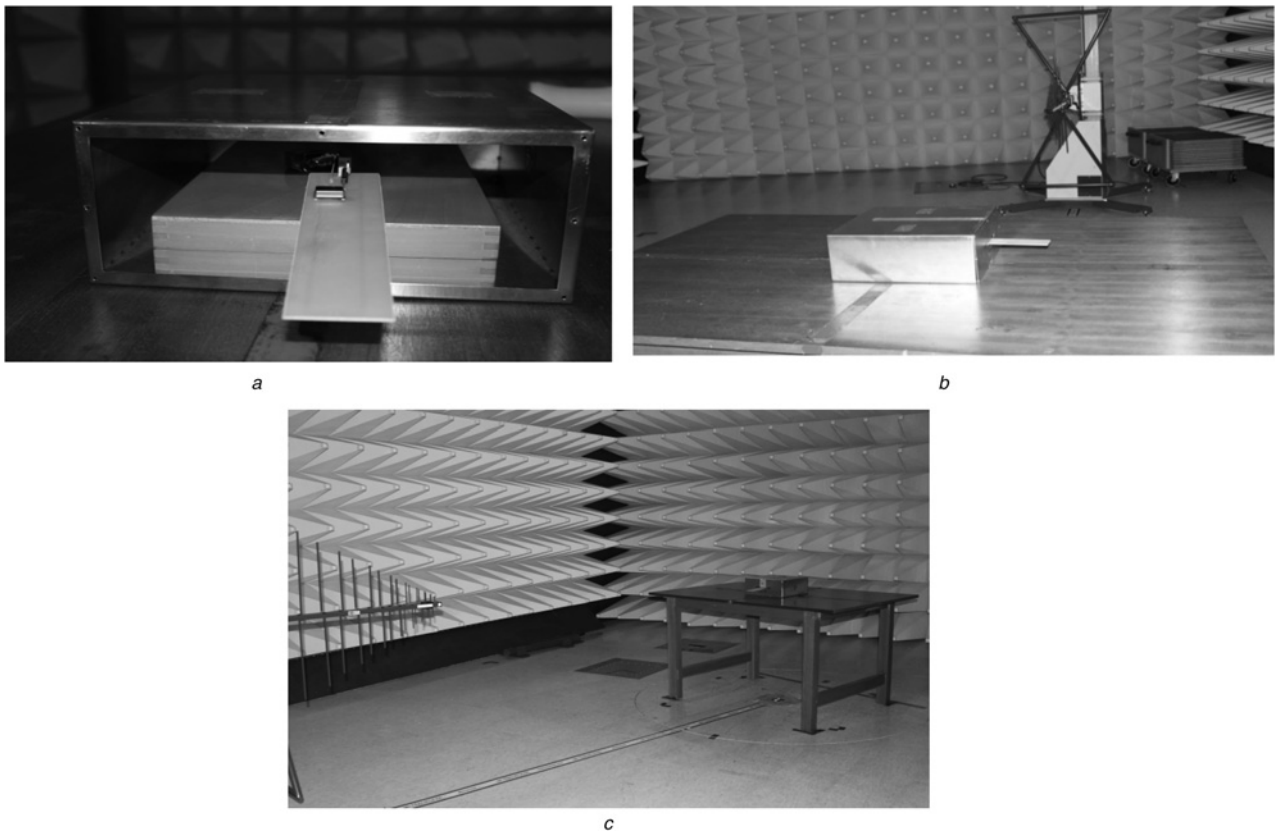

Fig. 6 *Regulator, oscillator, and their related connection traces*

a DUT placement in the shielding box
b DUT within shielding box in SAC
c DUT measurement set-up in SAC

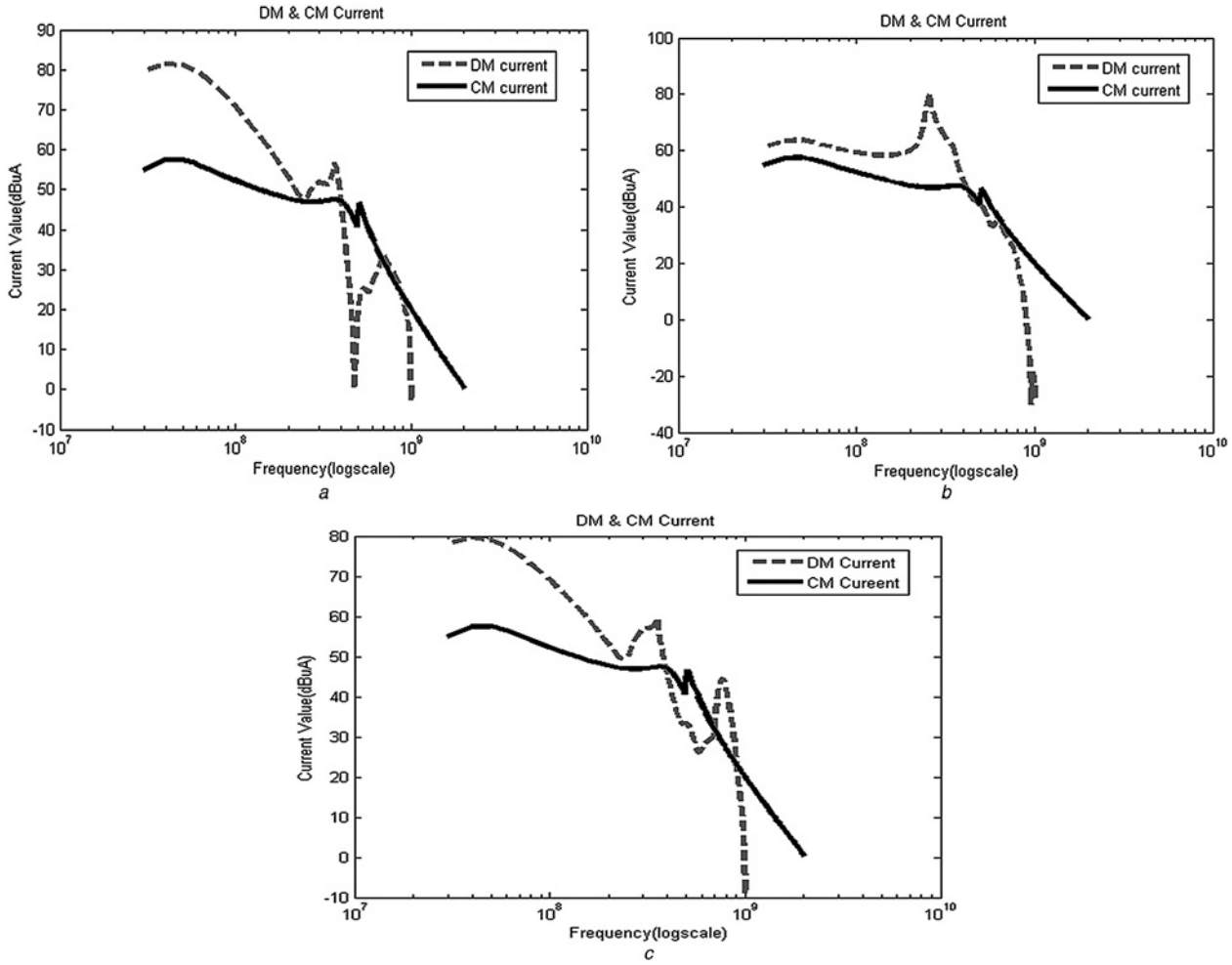

Fig. 7 *Prediction of PCB DM and CM currents*

a DM current versus CM current for short circuit
b DM current versus CM current for open circuit
c DM current versus CM current for 100 Ω load

5.2 Prediction of PCB CM and DM radiations

In theory, electrically long traces can be divided into identical electrically short segments. By observing this principle, DM RE for each segment was predicted from (1). The total radiation was then computed by superimposing the electric fields of all segments.

Although the predicted DM current was much larger than the predicted CM current as depicted in Fig. 7, the predicted CM radiation was, conversely, far higher than predicted DM radiation as demonstrated in Figs. 8 and 9. This is due to the cancellation effect between transmitting DM current and returning DM current.

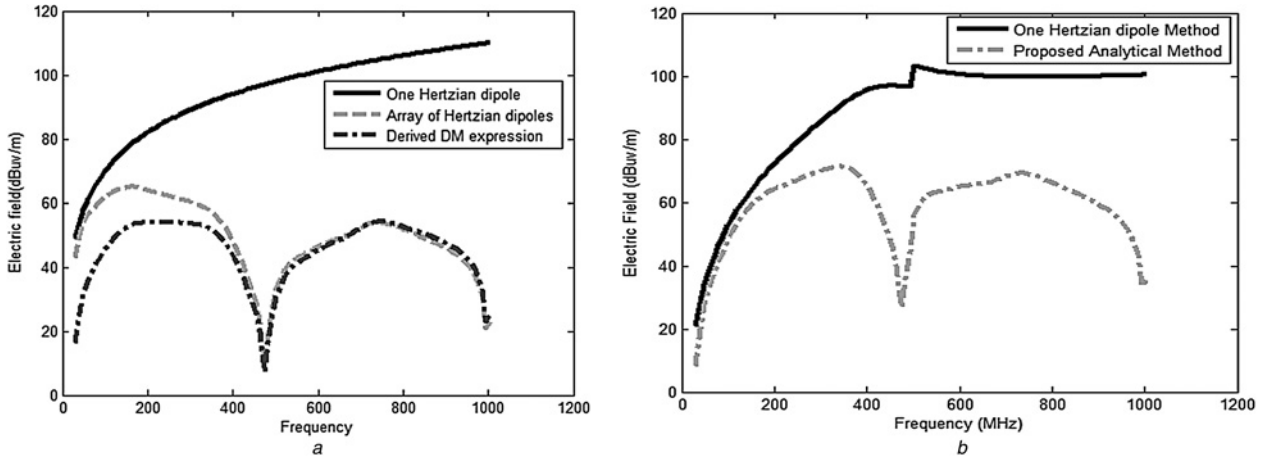

Fig. 8 *Prediction of PCB CM and DM radiations*

a DM radiations
b CM radiations both for short-circuit configuration, by the proposed method versus conventional method

IET Sci. Meas. Technol., 2016, Vol. 10, Iss. 1, pp. 28–37

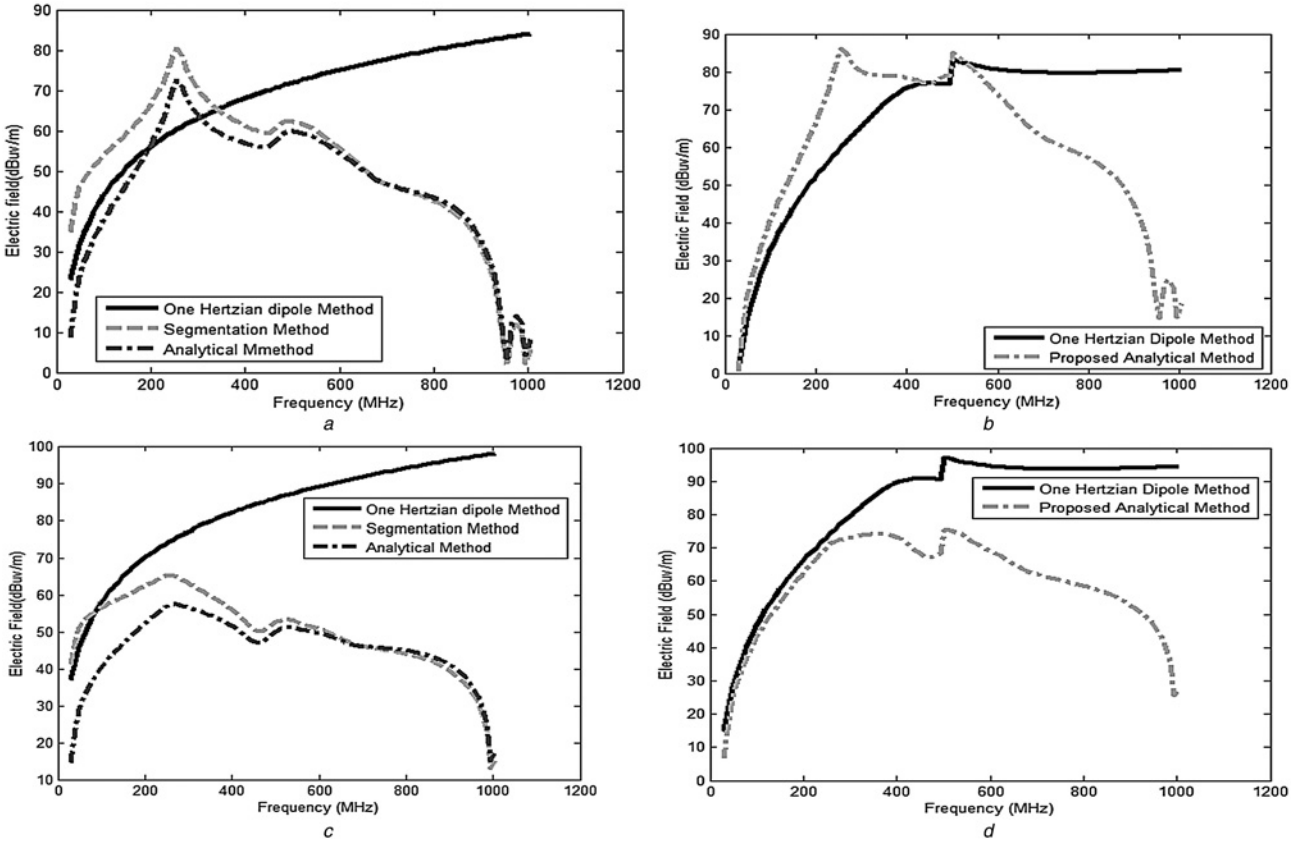

Fig. 9 *DM and CM radiations*

a DM radiations for open-circuit configuration
b CM radiations for open-circuit configuration
c DM radiations for 100 Ω configuration
d CM radiations for 100 Ω configuration by the proposed method versus conventional method

For this paper, two approaches have been employed to predict the DM and CM REs: the proposed method which applied (1) and (2) to all electrically short segments, and the conventional method that used (1) and (2) without segmentation and yields inaccurate results (the applications of (1) and (2) are presumably restricted to electrically short traces). Additionally, the analytical closed-form expressions were also derived to formulate the proposed method and then compared it with other methods. The results acquired from these methods were compared and validated against the measured results, as portrayed in Fig. 10.

Once again, three operating modes were considered: short circuit, open circuit, and 100 Ω load. By applying the proposed method for short-circuit configuration (Fig. 8), the DM radiation was about 20 dB and shifted slightly up to 60 dB at a certain frequency, then dropped slightly to 10 dB at another frequency (almost 480 MHz). This is possibly due to the standing wave current at that particular point. On the other hand, the DM radiation estimated using conventional method escalated exponentially, implying that an overestimated DM radiation for higher frequencies at which the traces become electrically long. As predicted, the CM radiation based on the proposed method was a bit higher than the DM radiation and it ranged between 20 and 60 dB. As for conventional method using (2), its CM radiation increased rapidly about 60 dB, soared above 100 dB at 480 MHz frequency, and continued with 100 dB at other higher frequencies.

In case of open-circuit configuration (Figs. 9*a* and *b*), the DM radiation for both proposed and conventional methods rose gradually from 25 to 80 dB. More precisely, the two methods exhibited similar behaviour up to 200 MHz (third harmonic of 66 MHz trapezoidal signal), the point at which trace length about one-tenth the wavelength. Visibly, the conventional method overestimated the DM radiation beyond 200 MHz owing to the limitation of (1) and (2), as discussed earlier, whereas the CM radiation estimated by the proposed method maintained above 60 dB across the frequency range, the CM radiations derived from conventional method soared from 20 to 80 dB, and then continued with 80 dB for the higher frequencies.

As for 100 Ω load configuration (Figs. 9*c* and *d*), the DM radiation by the proposed method remained above 40 dB and reached its peaks at 60 dB. Its distribution was similar to that of short-circuit configuration, except that it did not show a sharp decline at the same frequency. Notably, the CM radiation predicted by conventional model for all three operating modes manifested the same pattern, attributed to the modelling based on Hertzian antenna, in which the DM current is assumed to be uniform along the trace. By contrast, the CM radiation from the proposed method was modelled in accordance with non-uniform DM current distribution.

5.3 Prediction and measurement of total PCB REs

The predicted PCB REs were verified by comparing the measurement results as revealed in Fig. 10. The measured radiated electric fields did not exceed the prediction of upper bounds of the frequency range, which implied that the proposed prediction models are reliable for estimating REs from PCB traces. Moreover, they show better agreement with real measurement than predefined models computed from (1) and (2) without segmentation. To be specific, PCB REs for all three configurations were first predicted, and then validated by the measurements performed in the SAC. A good agreement between the prediction and measurement was consistently found except for higher frequencies. Such imperfection is ascribed to the fact that prediction models were developed based on (1) and (2) that are designated for electrically short traces associated with low-frequency range.

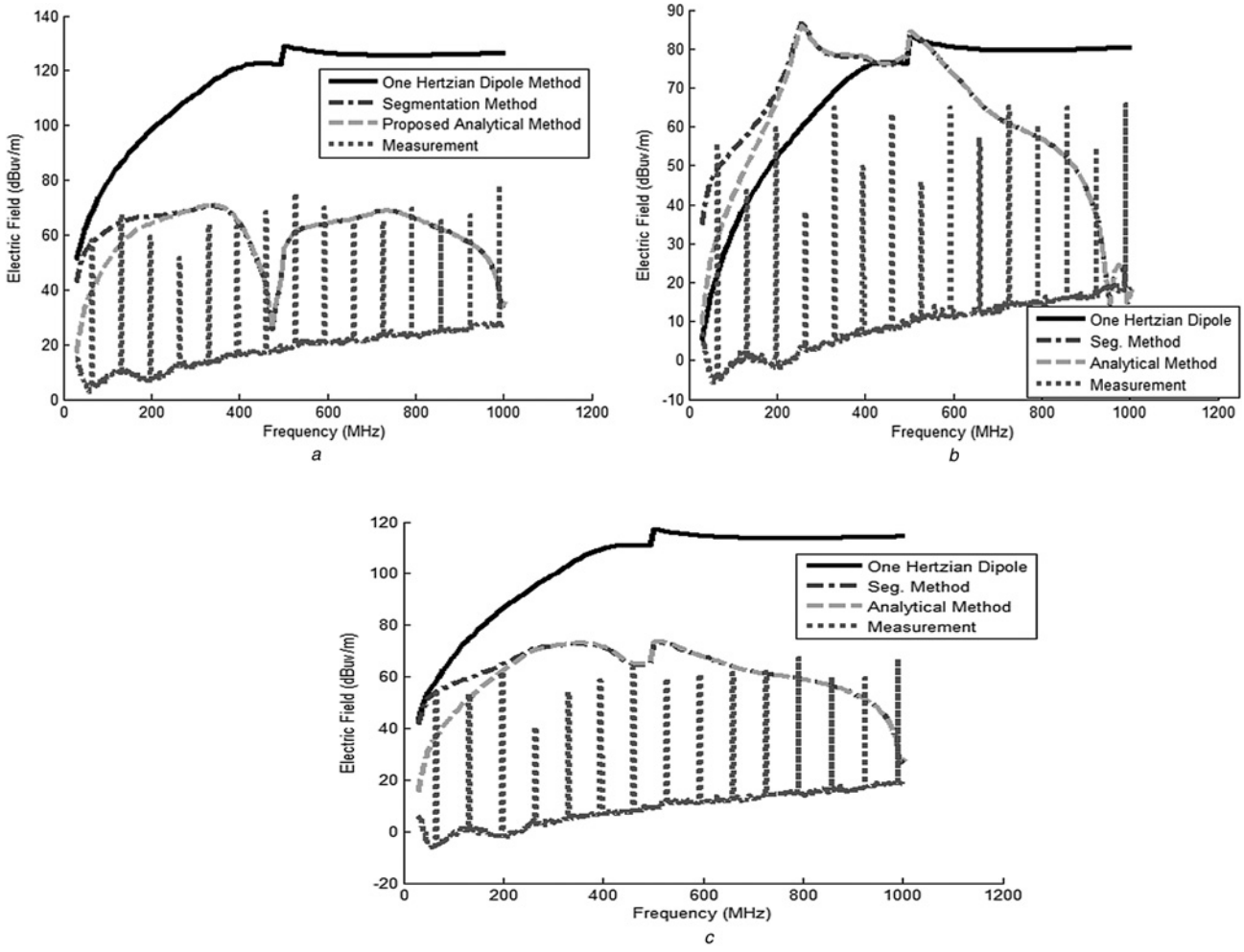

Fig. 10 *Predicted and measured total PCB REs for*

a Short circuit
b Open circuit
c 100 Ω load

Commonly, this method can be used for predicting maximum RE from PCB traces. However, two conditions must be fulfilled in order to apply this method with accurate results. The first condition is to ensure the operating current frequency is in the quasi-TEM frequency range as illustrated in Sections 2 and 3, whereas the second condition is related to the spherical angle (θ) that achieves the maximum RE. For traces longer than one wavelength, the angle (θ) must be scanned from 0° to 180°; therefore, the RE is computed at all angles. Then, the maximum RE can be estimated accurately. However, in this paper, the results demonstrated were limited to 2 GHz. This is because at 2 GHz, the trace length becomes one wavelength. For frequencies >2 GHz, the results are not accurate because the trace length becomes longer than one wavelength. This is attributed to the substitution of $\theta_{max} = 90^{\circ}$ which is valid for traces shorter than one wavelength. To extend this paper demonstration, a further and time-consuming computation process is required for the entire sphere to determine the maximum RE.

The accuracy and errors of the proposed method was discussed using many factors such as mean, mean absolute error (MAE), root mean square error (RMSE), and mean absolute percentage error (MAPE) as shown in Table 1. The measurement and modelling provide almost the same mean where the difference was about 1.5 dB. However, the error was 9.93% between measurement and modelling results. Generally, the proposed method estimates the maximum RE from PCB traces with accuracy 90.07% and this is a very good level of confidence. On the other hand, the uncertainties of measurement and modelling were 5.25 and 6.29 dB, respectively, which were acceptable from the measurement point of view. The uncertainty of measurement in SAC was due to many parameters such as receiver, frequency, antenna, table, and site imperfections.

Table 1 Accuracy and errors of the proposed model

Method	Factors				
	Mean, dB	MAE	RMSE	MAPE	Standard deviation
Measurement	55.51	—	—	—	5.25
analytical modelling	57.07	6.29	9.93%	8.77	5.28

Practically, the real PCB is populated with multiple traces. However, the RE can be computed using this method by calculating the maximum RE for all traces. Then, the REs from all t traces are superimposed to estimate the maximum total of RE.

6 Conclusion

This paper demonstrated the prediction of DM and CM REs from the high-speed PCB traces based on transmission-line theory and dipole antenna model methods. Additionally, the closed-form expressions were also derived to predict the DM and CM RE of electrically long PCB traces. The theoretical results presented in this paper clearly showed that our equations improved the limitations of the formulations for electrically short PCB traces. The reliability of these prediction models was confirmed by comparing the predicted results with the measured results. Although favourable agreement

IET Sci. Meas. Technol., 2016, Vol. 10, Iss. 1, pp. 28–37

was generally perceived in the results, it can be said that these prediction models are, however, less accurate at 2 GHz and above. Certainly, improvements can be made to enhance the development of software tools that can efficiently characterise, quantify, and predict PCB REs.

7 Acknowledgments

The authors to acknowledge and express sincere appreciation to the Universiti Tun Hussein Onn Malaysia (UTHM) for financing the research project under the University Contract Research Grant Scheme. The support given by Research Centre for Applied Electromagnetics, UTHM for providing the facilities to perform this research is also highly appreciated.

8 References

1 Montrose, M.: 'Printed circuit board design techniques for EMC compliance – a handbook for designers' (IEEE Press/Wiley Interscience, New York, 1999, 2nd edn. 2000)
2 Paul, C.R.: 'Introduction to electromagnetic compatibility' (Wiley Interscience, New Jersey, 1992, 2nd edn. 2006)
3 Ott, H.W.: 'Electromagnetic compatibility engineering' (John Wiley & Sons, New Jersey, 2009, 1st edn.)
4 Leone, M.: 'Closed-form expressions for the electromagnetic radiation of microstrip signal traces', *IEEE Trans. Electromagn. Compat.*, 2007, **49**, (2), pp. 322–328
5 Chen, I.-F., Peng, C.-M., Hsue, C.-W.: 'Circuit-concept approach to radiated emissions of printed circuit boards', *IEE Proc. Sci. Meas. Technol.*, 2004, **151**, (3), pp. 205–210
6 Watanabe, T., Wada, O., Miyashita, T.: 'Common-mode current generation caused by difference of unbalance of transmission lines on a printed circuit board with narrow ground pattern', *IEICE Trans. Commun.*, 2000, **E83-B**, (3), pp. 593–599
7 Su, C., Hubing, T.H.: 'Imbalance difference model for common-mode radiation from printed circuit boards', *IEEE Trans. Electromagn. Compat.*, 2011, **53**, (1), pp. 150–156
8 Zhang, N., Kim, J., Ryu, S., *et al.*: 'Prediction of common-mode radiated emission of PCB with an attached cable using imbalance difference model', *IEICE Trans. Commun.*, 2015, **E98-B**, (4), pp. 638–645
9 Sasabe, K., Bullivant, A., Yoshida, K., *et al.*: 'Prediction of electric far-field strength from printed circuit boards by measuring the common-mode current'. Proc. IEEE Int. Symp. on Electromagnetic Compatibility, Washington, August 2000, pp. 379–384
10 Wang, J., Sasabe, K., Fujiwara, O.: 'A simple method for predicting common-mode radiation from a cable attached to a conducting enclosure', *IEICE Trans. Commun.*, 2002, **E85-B**, (7), pp. 1360–1367
11 Park, H.H., Park, H., Lee, H.S.: 'A simple method of estimating the radiated emission from a cable attached to a mobile device', *IEEE Trans. Electromagn. Compat.*, 2013, **55**, (2), pp. 257–264
12 Ramo, T.S., Whinnery, J., Duzer, V.T.: 'Fields and waves in communication electronics' (John Wiley & Sons, New York, 1984, 3rd edn. 1994)
13 Balanis, C.A.: 'Antenna theory: analysis and design' (John Wiley & Sons, New Jersey, 2005, 3rd edn. 2012)
14 Shim, H.W., Hubing, T.H.: 'Derivation of a closed-form approximate expression for the self-capacitance of a printed circuit board trace', *IEEE Trans. Electromagn. Compat.*, 2005, **47**, (4), pp. 1004–1008
15 King, R., Harrison, C.W.: 'The distribution of current along a symmetrical center-driven antenna', *Proc. IRE*, 1943, **31**, (10), pp. 548–567
16 King, R.: 'Asymmetrically driven antennas and sleeve dipole', *Proc. IRE*, 1950, **38**, (10), pp. 1154–1164
17 Schelkunoff, S., Friis, H.: 'Antenna: theory and practice' (John Wiley & Sons, New York, 1951)